

线源扩散的模拟计算*

程紫润 傅大放

(东南大学环境工程研究所, 南京 210018)

摘要 在传统的高斯扩散理论上, 提出了一种计算线源扩散的方法: 将公路线源分成若干存在初期扩散的单元, 每个单元近似成一个过单无中心点与风向垂直的短线源, 它的扩散按高斯垂直风模式计算, 测点的浓度是若干子线源的贡献之和。与 CLINE2 等模式相比, 该方法对任意风向有限长线源都适用, 而且可进行一条公路上有不同源强路段的计算。模式的计算结果与现场示踪及尾气污染的实测数据吻合较好。

关键词 线源, 污染, 模拟计算。

公路尾气扩散模式都是以高斯模式为基础, 如 HIGHWAY- I、CLINE2 模式^[1,2]。平坦地形上的公路, 可以假设为无限长线源, 横风向产生的浓度相等; 当风向与线源垂直时, 连续排放的线源的高斯扩散模式为:

$$c(x, y, z, H) = \frac{q}{\sqrt{2\pi u \sigma_z}} \cdot \left\{ \exp\left[-\frac{(z-H)^2}{2\sigma_z^2}\right] + \exp\left[-\frac{(z+H)^2}{2\sigma_z^2}\right] \right\} \quad (1)$$

对风向与线源成任意角度、实际线源的“边缘效应”等问题如何解决, HIGHWAY- I、CLINE2 模式取得了一些进展, 但模式中的扩散参数仍未考虑行车机械扰动等因素的影响, 在实际应用中还存在计算工作量大等方面的问题^[3,4]。本文在高斯线源扩散模式计算方面作了一些探讨, 模式中的源强及扩散参数的计算方法另文详述。

1 计算模式

1.1 建立模型的基本假设

模式建立在风向与线源垂直的高斯模式基础上, 因此要满足如下假设条件:

(1) 污染物浓度在垂直方向和横风向的分布符合高斯分布;

(2) 在全部空间中风速是均匀、稳定的;

(3) 源强是连续的;

(4) 在扩散过程中污染物质量守恒。

1.2 物理模型

尾气扩散过程存在一初期扩散混合区, 其宽为 W_0 (路宽加 3m)。将线源分为宽为 W_0 的若干单元, 下风向测点的浓度看作是所有单元的贡献之和。再将每个单元近似成一过单元中心点沿风向法线方向的有限长线源(子线源), 子线源的长度和风向与路段夹角 φ 有关(见图 1、图 2)。

1.3 模式数学推导

子线源每一微段 d_y 对测点的浓度贡献 d_c , 按式(1)计算:

$$d_c = \frac{q d_y}{2\pi u \sigma_y \sigma_z} \cdot \exp\left(-\frac{y^2}{2\sigma_y^2}\right) \cdot \left\{ \exp\left[-\frac{(z-H)^2}{2\sigma_z^2}\right] + \exp\left[-\frac{(z+H)^2}{2\sigma_z^2}\right] \right\} \quad (2)$$

因 σ_z 与 y 无关, 令 $A = \left\{ \exp\left[-\frac{(z-H)^2}{2\sigma_z^2}\right] + \exp\left[-\frac{(z+H)^2}{2\sigma_z^2}\right] \right\}$, 子线源对测点的浓度贡献可简化成 5 小段计算, 如图 3 所示。

每一小段的浓度贡献:

$$c = \frac{Aq}{2\pi u \sigma_y \sigma_z} \cdot \int_{y_1}^{y_2} \exp\left(-\frac{y^2}{2\sigma_y^2}\right) d_y \quad (3)$$

$$\text{令 } P = \frac{y}{\sigma_y}$$

* 国家自然科学基金资助项目

1993 年 7 月 14 日收到修改稿

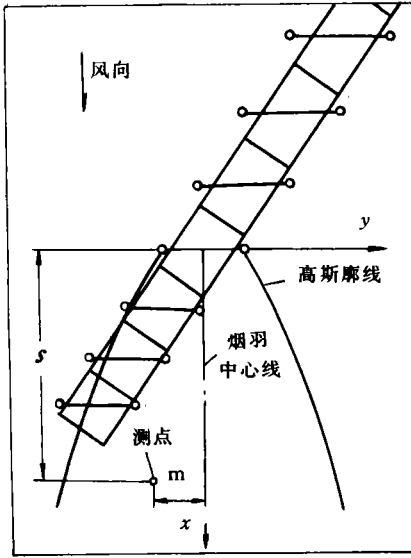


图1 任意风向有限长线源计算方法示意图

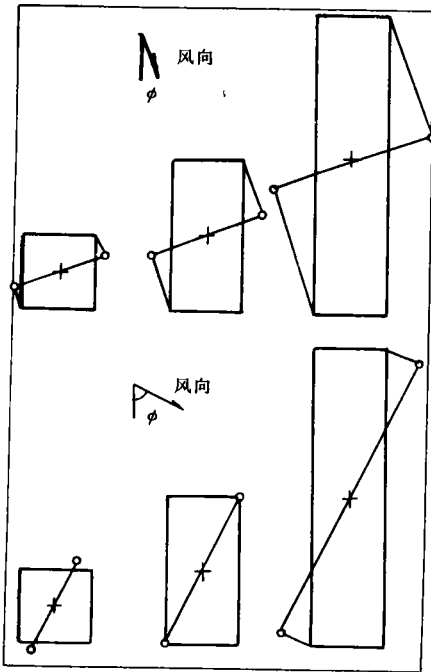


图2 子线源长度与风向的关系

$$\begin{aligned}
 \text{则 } c &= \frac{Aq}{2\pi u \sigma_y \sigma_z} \int_{y_1/\sigma_y}^{y_2/\sigma_y} \exp\left(-\frac{P^2}{2}\right) \sigma_y dP \\
 &= \frac{Aq}{\sqrt{2\pi} u \sigma_z} \cdot PD \quad (4)
 \end{aligned}$$

其中, $PD = \frac{1}{\sqrt{2\pi}} \int_{y_1/\sigma_y}^{y_2/\sigma_y} \exp\left(-\frac{P^2}{2}\right) dP$

对第 i 个子线源的第 j 小段

$$\begin{aligned}
 PD_{ij} &= \frac{1}{\sqrt{2\pi}} \int_{y_j/\sigma_{y_i}}^{y_{j+1}/\sigma_{y_i}} \exp\left(-\frac{P^2}{2}\right) dP \\
 c_{ij} &= \frac{Aq_j}{\sqrt{2\pi} u \sigma_{z_i}} \cdot PD_{ij} \quad (5)
 \end{aligned}$$

第 i 个子线源的浓度贡献:

$$\begin{aligned}
 c_i &= \sum_{j=1}^5 \frac{Aq_j}{\sqrt{2\pi} u \sigma_{z_i}} PD_{ij} \\
 &= \frac{A}{\sqrt{2\pi} u \sigma_{z_i}} \cdot \sum_{j=1}^5 (WT_j \cdot q_j \cdot PD_{ij}) \quad (6)
 \end{aligned}$$

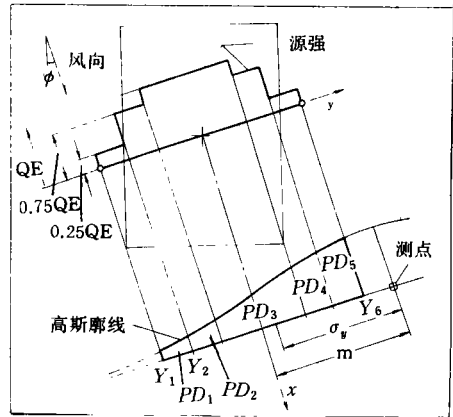


图3 子线源简化计算示意图

WT_j 为每一小段的源强权重, q_j 为每一子线源的源强。其中:

$$WT_1 = WT_5 = 0.25 \quad (7)$$

$$WT_2 = WT_4 = 0.75 \quad (8)$$

$$WT_3 = 1 \quad (9)$$

$\sigma_{y_i}, \sigma_{z_i}$ 与测点至第 i 个子线源的垂直距离 S_i 有关, S_i 由下式确定:

$$S_i = D \sin \phi + L_i \cos \phi \quad (10)$$

$$L_i = 12 \varepsilon_i + \sum_{k=1}^{i-1} \varepsilon_k \quad (11)$$

式中, ε_i —— 第 i 单元的长度;

L_i —— 第 i 单元中心点至起始计算点的距离; D —— 测点至公路线源的垂直距离。

为了在保证计算精度的前提下提高计算速度, 离测点越远的单元可以取得越长:

$$\varepsilon_i = W_0 \beta^{-1}$$

通过计算比较, β 可按表 1 确定。

PD_{ij} 可以近似成一个 5 次多项式:

表 1 计算单元增长因子

φ	$\varphi \leq 20^\circ$	$20^\circ < \varphi \leq 50^\circ$	$50^\circ < \varphi \leq 70^\circ$	$70^\circ < \varphi$
β	1.1	1.5	2.0	4.0

$$PD_{ij} = 0.3989 \exp(ARG) \cdot (0.3194T - 0.3566T^2 + 1.7815T^3 - 1.8215T^4 + 1.3303T^5) \quad (12)$$

式中, $ARG = -\frac{LIM^2}{2}$

$$T = \frac{1}{1 + 0.23164LIM}$$

$$LIM = |y_i| / \sigma_{yi}$$

测点到每一小段起始点的距离 y_i 可通过座标关系确定:

$$m_i = D \cos \varphi - L_i \sin \varphi \quad (13)$$

$$n_i = \varepsilon_i \sin \varphi + W_0 \cos \varphi \quad (14)$$

$$EM_i = |\varepsilon_i \sin \varphi - W_0 \cos \varphi| \quad (15)$$

$$EN_i = \frac{1}{2} (n_i - EM_i) \quad (16)$$

$$y_1 = m_i + \frac{1}{2} n_i \quad (17)$$

$$y_2 = y_1 - \frac{1}{2} EN_i \quad (18)$$

$$y_3 = y_2 - \frac{1}{2} EN_i \quad (19)$$

$$y_4 = y_3 - EM_i \quad (20)$$

$$y_5 = y_4 - \frac{1}{2} EN_i \quad (21)$$

$$y_6 = y_5 - \frac{1}{2} EN_i \quad (22)$$

式中, y_i 为测点沿子线源方向距每 1 节点距离; m_i 为测点沿子线源方向到单元中心点距离; n_i 为子线源长度; EM_i 为子线源中间 1 小段长度; $\frac{1}{2} EN_i$ 为子线源两侧 4 小段的每段长度。

测点浓度是所有子线源的贡献和:

$$c = \frac{1}{2\pi u} \sum_{i=1}^n \left\{ \frac{1}{\sigma_{zi}} \left[\exp\left(-\frac{(z+H)^2}{2\sigma_{zi}^2}\right) + \exp\left(-\frac{(z-H)^2}{2\sigma_{zi}^2}\right) \right] \cdot \sum_{j=1}^5 (WT_j \cdot q_j \cdot PD_{ij}) \right\} \quad (23)$$

测点浓度是上风向路段及下风向路段的总贡献, 应分别计算后求代数之和。式中 n 可根据路段长度确定:

$$\sum_{i=1}^n \varepsilon_i \leq UL(DL) \quad (24)$$

式中, UL ——上风向路段总长度;

DL ——下风向路段总长度。

计算测点下风向路段的浓度贡献或计算上风向测点浓度时(图 4), 有关变量计算的变化如下:

$$S_i = L_i \cos \varphi - D \sin \varphi \quad (25)$$

$$m_i = L_i \sin \varphi + D \cos \varphi \quad (26)$$

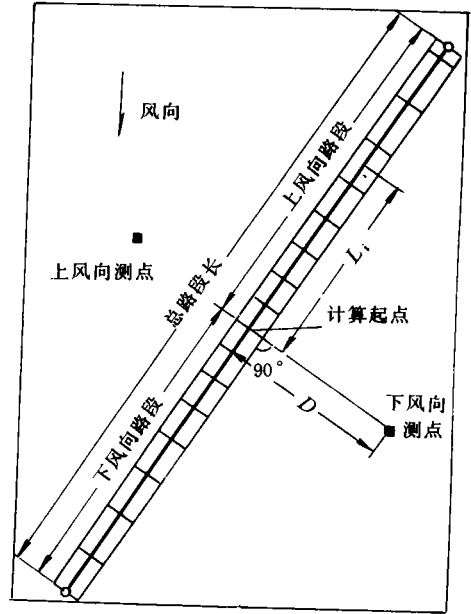


图 4 测点上、下风向路段与公路上、下风向测点

2 模式验证

用该模式计算北京京顺公路示踪剂浓度分布及沪嘉高速公路尾气(CO)浓度分布, 计算值与实测值吻合较好(表 2、表 3)。

与 CLINE2、HIGHWAY-II 模式的计算值对照, 该模式的计算结果更接近实测值。

该模式在 φ 较小, 甚至在 $\varphi = 0^\circ$ 时, 计算值与实测值仍有较好的相关性。

3 讨论

与其它高斯线源扩散模式的计算方法相比该方法有以下特点:

- (1) 没有作无限长线源的假设;
- (2) 在风向与路段夹角很小时没有作近似处

理;

特点;

(3)没有复杂的积分计算;

(5)可以进行一条公路上有不同源强路段情

(4)虚拟线源比虚拟点源更接近实际线源的

况下的计算;

表 2 京顺公路示踪剂浓度实测值与计算值(mg/m³)

时间	计算与实测值	10m	50m	100m	150m	200m	R	S _{XY} /X̄
1988-12-24	HIGHWAY- I 计算值	4.92	1.76	1.27	1.05	0.096	0.88	0.30
	计算值	3.97	2.13	1.86	1.15	1.03	0.85	0.25
	实测值	3.81	1.82	1.94	0.09	2.15		
1989-07-19	HIGHWAY- I 计算值	3.74	0.97	0.54	0.39	0.03	0.99	1.55
	计算值	4.37	2.26	1.09	0.58	0.21	0.98	0.62
	实测值	6.90	2.40	1.30	0.12			

表 3 沪嘉高速公路 CO 分布计算值与实测值(mg/m³)

样本号	计算与实测值	15m	25m	55m	75m	95m	R	S _{XY} /X̄
116 (45°)	CLINE2 计算值	1.94	1.97	1.98	1.97	1.96	0.87	0.62
	计算值	1.65	2.62	3.25	1.86	1.75	0.89	0.11
	实测值	1.30	2.90	3.20	1.53	2.35		
117 (0°)	CLINE2 计算值	0.051	0.085	0.086	0.075	0.069	无相关性	
	计算值	0.95	0.83	0.70	0.69	0.59	0.95	0.022
	实测值	0.87	0.77	0.74	0.59	0.69		
118 (90°)	CLINE2 计算值	1.91	1.96	1.98	1.97	1.96	0.51	1.64
	计算值	1.93	3.02	3.58	2.03	1.91	0.82	0.21
	实测值	1.71	3.93	3.99	1.95	1.87		
210 (67°)	CLINE2 计算值	1.60	1.69	1.69	1.68	1.66	0.88	0.18
	计算值	1.35	1.42	1.52	1.79	1.63	0.85	0.25
	实测值	2.46	1.40	1.49	1.86	1.65		

(6)对路堑的情况,仍可按本方法计算,但平面上初期扩散混合区的源强与实际源强有一定的稀释度。

参考文献

- 1 Petersen W B. User' s Guide for Highway- I —— A Highway Air Pollution Model. EPA-600/8-80-018
- 2 David P Choc. Atmospheric Environment. 1978, 12(1):823
- 3 孙锡平等. 交通环保. 1986, 6; 2
- 4 曹文俊等. 南京气象学院学报. 1991, 14(2):203

(上接第 37 页)浓度越低。

(3)甲酸甲酯的生成温度曲线和消失温度曲线出现了明显变化, Ce-O/r-Al₂O₃ 的 2 值较大, 故出现了 1 个峰, 但总趋势自左至右渐次降低, 32 号催化剂以后的两温度曲线都分别低于 130℃ 和 180℃。而且 2 者之间的距离越来越接近, 最窄时只有 70℃ 左右。故甲酸甲酯的伴生区间随催化剂活性增加而变窄。

者靠的很近, 大约相差只有 20—30℃ 左右, 并且远离消失温度曲线, 这说明 32—41 号催化剂在对甲醇氧化时, 在一个比较窄的温度区间内, 甲醛和甲酸甲酯的伴生浓度达到最大, 然后迅速降低到 50×10⁻⁶ 以下, 如果把 50×10⁻⁶ 以下的甲酸甲酯或甲醛完全氧化, 则需要更高的温度。

参考文献

- 1 Foster R E. Oil and Gas Journal. Mar h, 1980, 30
- 2 Grimm R A. S. A. E. 1980. No. 800053
- 3 王金安, 汪仁. 环境科学. 1994, 15(2): 45
- 4 卢冠忠, 汪仁. 催化学报. 1991, 12(4):261

(4)对于 32—41 号催化剂对应的甲醛及甲酸甲酯的峰值温度曲线和生成温度曲线, 发现 2

Abstracts

Chinese Journal of Environmental Science

formate, deep oxidation, catalyst.

Study on the Recovery of Carbon Monoxide (CO) from Industrial Exhaust Gases by a Chemical Absorption Method. Su Chunhui, Che Yinchang et al. (Dept. of Nonferrous Metal., Northeastern University, Shen' yang 110006); *Chin. J. Environ. Sci.*, **15**(3), 1994, pp. 38—41

An aqueous CuCl-MgCl_2 system has been found to be a preferred, highly selective CO absorbent. A relationship between the maximum capacity of the absorbent to absorb CO and temperature was determined. The effects of a change in exhaust gas composition on CO recovery was also studied. The CO recovery with this absorption process was found to be up to 93%, and the recovered CO has a purity of 98% as determined by gas chromatography (GC). The CO gas can be desorbed from the CO absorbed absorbent liquor at temperatures in the range of 120—140 °C. In addition, the mechanism of the absorption reaction between CO and the aqueous CuCl-MgCl_2 absorbent system was preliminarily studied. The new process can be used to separate and recover CO gas from industrial exhaust gases, such as the off-gas from steelmaking converters.

Key words: carbon monoxide, absorbent, chemical absorption

Atmospheric Dispersion Parameters for High Overhead Pollution Sources Fitted with the Monitored Data from Various Parts of China. Gu Yongrui, Zhang Tong, Wang Dongpu (Inner Mongolian Central Monitoring Station for Environmental Protection, Huhehaote 010010); *Chin. J. Environ. Sci.*, **15**(3), 1994, pp. 42—46

In a calculation of the atmospheric dispersion of emissions from a high overhead source, the atmospheric dispersion parameters given in the National Standards GB3840-91 and the Briggs parameters were found to be no longer suitable. By using the general expression for the Briggs atmospheric dispersion parameters ($\sigma = \alpha x (1 + \beta x)^{-1/2}$) to fit the atmospheric dispersion parameters which were actually measured in various parts of China, the fitted parameters were obtained and were found more reasonable as compared with the GB3840-91 and Briggs parameters, and thus have a practical value in use for calculating other atmospheric dispersion parameters.

Key words: atmospheric dispersion, fitting, high overhead sources.

Determination of the Source Intensity of the Gases Released from Municipal Solid Wastes Dumping sites and Their Environmental Impact Assessment. Zhou Zhongping, Zhang Jun (Dept. of Environ. Eng.,

Tsinghua University, Beijing 100084); *Chin. J. Environ. Sci.*, **15**(3), 1994, pp. 47—52

After taking samples of the gases released from the Beishenshu Municipal Solid Wastes Dumping Site in Beijing and making the qualitative and quantitative analyses of the samples, two methods were used to study the determination of the intensity of the gases releasing sources, by which an assessment was made on the environmental impact of the gases emitted from the dumped garbage. Some countermeasures feasible to control such a pollution were suggested.

Key words: gases release, garbage dumping site, source intensity, EIA.

Forms and Transformation of Chromium Species in Soils. Chen Yingxu, He Zeng' yao et al. (Dept. of Environmental Protection, Zhejiang University of Agriculture, Hangzhou 310029); *Chin. J. Environ. Sci.*, **15**(3), 1994, pp. 53—56

By developing a method for the fractional extraction of chromium species in various binding states in soil, it was found that the extractants of 1 mol/L NH_4Ac , 2 mol/L HCl and 5% H_2O_2 -2mol/L HCl in use for a sequential extraction of chromium species from soil can give the exchangeable Cr species, precipitated Cr species, and organics-bound Cr species, respectively. The results show that in the natural soil the Cr species are present dominantly in a precipitated or residual state. Under the reducing conditions, the Cr species in soil tend to be transformed into those in an organics-bound state. As the soil pH value was lowered, the levels of water soluble Cr species and exchangeable Cr species raised while the levels of Cr species in precipitated or residual state being reduced. The soil pH value can be lowered by adding Cr(III) species and raised by adding Cr(VI) species.

Key words: chromium, soil, fractional extraction, species transformation.

Mathematical Modelling on the Dispersion of Line Sources of Air Pollution. Cheng Zirun, Fu Dafang (Institute of Environmental Engineering, Southeast University, Nanjing 210018); *Chin. J. Environ. Sci.*, **15**(3), 1994, pp. 57—60

Based on the traditional Gaussian dispersion theory, a method has been proposed to calculate the dispersion of line sources of air pollution caused by vehicles running on road. In this method, a road line source is divided into several elements in which an initial dispersion exists; each of the elements is considered to be a proximate short line source which is passing through the midpoint of the element and is rectangular to the direction of wind, and can be calculated for its dispersion based on the Gaussian Model for rectangular wing, with the concentration

Abstracts

Chinese Journal of Environmental Science

of pollutants at a measuring site being a sum of the contributions from all the short line sources divided. As compared with other models such as CLINE2, this method is applicable to all the line sources of finite length in an arbitrary wind direction and can be used to calculate for a reach with different intensities of sources on a road. The results of modelling calculations are consistent well with the data from field tracing and really measuring the pollution by vehicles exhausts.

Key words: line source, air pollution, modelling calculation.

Effects of exhaust gas from diesel vehicles on urban air quality. Yao Weixi, Zhang jinchun et al. (Research Center for Eco-Environmental Sciences, Chinese Academy of Sciences, Beijing 100085); *Chin. J. Environ. Sci.*, **15**(3), 1994, pp. 61—64

The changes in the concentration of polycyclic aromatic hydrocarbons (PAHs) in exhaust gas emitted from diesel vehicles under different working conditions and their effects on urban air quality were reported in this paper. The PAHs emissions were found to be related to the types of engine and their conditions, with the lowest emission generated upon an operation load of between about 2%—5%. Cyclopenta (c,d)pyrene was measured respectively in the exhaust gases and urban air, and was found to have a much higher mutagenicity than benzo(a)pyrene.

Key words: diesel vehicles, polycyclic aromatic hydrocarbons, air quality, cyclopenta (c,d)pyrene.

Extraction and Synchronous Fluorescent Spectrometry for the Determination of Benzo (a) pyrene in Airborne Particulates. Lei Shihuan, Zhao Zhenhua (Beijing Municipal Research Institute of Environmental Protection, Beijing 100037); *Chin. J. Environ. Sci.*, **15**(3), 1994, pp. 65—67

A rapid and effective method for detecting benzo(a)pyrene in airborne particulates was developed, in which benzo(a)pyrene was extracted in one minute step with concentrated sulfuric acid from a cyclohexane extracted solution from the airborne particulates, and then determined with a synchronous fluorescent spectrometry. The best results were obtained at $\Delta\lambda$ of 20nm. Benzo(a)pyrene in the concentrated sulfuric acid phase was stable within 1 hour. The recovery was found to be 85% for 0.10 μg of benzo(a)pyrene standard. No interference with other polynuclear aromatic hydrocarbons was found in the range of 530—600 nm of synchronous fluorescent spectra. For a comparison, the samples were also determined by using the unified method of acetylated paper TLC/ fluorescent photospectrometry, with the results in a variance of 15% between

both methods. The analytical cycle for the present method can shorten by 1 hour.

Key words: benzo (a) pyrene, synchronous fluorescent spectrometry, extraction, airborne particulates.

Plasma Decomposition of Sulfur Dioxide (SO₂). Yi Chengwu, Liu Hengquan, Bai Xiyao et al. (Anshan Research & Design Institute of Electrostatic Technology, Anshan 114011); *Chin. J. Environ. Sci.*, **15**(3), 1994, pp. 68—70

The results were reported for the decomposition of the noxious gas SO₂ by using a plasma technique under the conditions of ambient temperature and atmospheric pressure. The effects of SO₂ concentrations, gas flow rates and furnace temperatures on the decomposition of SO₂ were examined and a comparison was made for the energy consumption of SO₂ decomposition and the amount of SO₂ decomposed by the plasma generated by pulse-superposed positive or negative DC voltages. The results show that this process has a much lower energy consumption and a higher rate of SO₂ decomposition, with 1.61—1.97 kg of SO₂ decomposed per kW · h of electric power at a decomposition rate of over 80%.

Key words: plasma, decomposition, sulfur dioxide, high voltage pulse.

Study on the Method for Detecting Environmental Toxicants and Its Application; Bacterial Culture/ Head Space Gas Chromatography. Cheng Jinqun et al. (Shenzhen Public Health and Anti-epidemic Station, Shenzhen 518020); *Chin. J. Environ. Sci.*, **15**(3), 1994, pp. 71—74

Aiming to explore a rapid, sensitive method for monitoring environmental toxicants, a head space gas chromatographic technique was used to determine the extent to which the environmental toxicants have inhibited carbon dioxide (CO₂) as a product of the bacteria *E. Coli* metabolism and IC₅₀, a concentration of an environmental toxicant being tested that has an effect of 50% inhibition, was used as a measure of the toxicity of the environmental toxicant. The optimized conditions in this test include, a bacteria concentration of 10⁹/ml, pH 7.2—7.4, a ratio of gas/liquid of 1 : 2.5 in head space tube, a culture time of 4 hours, and the operation conditions of chromatograph suitable for CO₂ determination. This method has been used to test the toxicities of 8 ions, with an order of decreasing toxicity in terms of IC₅₀ value as follows; Hg²⁺ (0.86 ppm), Cu²⁺ (8.00 ppm), Cd²⁺ (8.39 ppm), CN⁻ (10.20 ppm), Pb²⁺ (11.20), Zn²⁺ (15.20 ppm), Sn²⁺ (20.10 ppm), Ni²⁺ (39.70 ppm). The joint toxicities among Cd²⁺, Hg²⁺, Cu²⁺, Zn²⁺ and CN⁻